

First-principles study of ferroelectricity and isotope effects in H-bonded KDP crystals

S. Koval⁽¹⁾, J. Kohanoff,⁽²⁾ J. Lasave⁽¹⁾, G. Colizzi⁽²⁾, and R. Migoni⁽¹⁾

⁽¹⁾ *Instituto de Física Rosario, Universidad Nacional de Rosario,
27 de Febrero 210 Bis, 2000 Rosario, Argentina.*

⁽²⁾ *Atomistic Simulation Group, The Queen's University, Belfast BT7 1NN, Northern Ireland.
(March 22, 2022)*

By means of extensive first-principles calculations we studied the ferroelectric phase transition and the associated isotope effect in KH_2PO_4 (KDP). Our calculations revealed that the spontaneous polarization of the ferroelectric phase is due to electronic charge redistributions and ionic displacements which are consequence of proton ordering, and not vice versa. The experimentally observed double-peaked proton distribution in the paraelectric phase cannot be explained by a dynamics of only protons. This requires, instead, collective displacements within clusters that include also the heavier ions. These tunneling clusters can explain the recent evidence of tunneling obtained from Compton scattering measurements. The sole effect of mass change upon deuteration is not sufficient to explain the huge isotope effect. Instead, we find that structural modifications deeply connected with the chemistry of the H-bonds produce a feedback effect on tunneling that strongly enhances the phenomenon. The resulting influence of the geometric changes on the isotope effect agrees with experimental data from neutron scattering. Calculations under pressure allowed us to analyze the issue of universality in the disappearance of ferroelectricity upon compression. Compressing DKDP so that the distance between the two peaks in the deuteron distribution is the same as for protons in KDP, corresponds to a modification of the underlying double-well potential, which becomes 23 meV shallower. This energy difference is what is required to modify the O-O distance in such a way as to have the same distribution for protons and deuterons. At the high pressures required experimentally, the above feedback mechanism is crucial to explain the magnitude of the geometrical effect.

I. INTRODUCTION.

Potassium dihydrogen phosphate (KH_2PO_4 , or KDP) crystals are a key component in quantum electronics. They are widely used in controlling and modulating the frequency of laser radiation in optoelectronic devices, amongst other uses such as TV screens, electrooptic deflector prisms, interdigital electrodes, light deflectors, and adjustable light filters. Besides the obvious technological interest, KDP is also interesting from a fundamental point of view. KDP is a prototype ferroelectric (FE) crystal belonging to the family of hydrogen-bonded ferroelectrics, which was extensively studied in the past.^{1,2} Their PO_4 molecular units are linked by hydrogen bonds, and ferroelectricity appears to be connected to the behavior of the protons in these H-bonds. Normal (H_2O) ice is the most prominent member of this family,^{3,4} which also includes other compounds like PbHPO_4 ,⁵ and squaric acid ($\text{C}_4\text{H}_2\text{O}_4$).⁶ What makes KDP particularly interesting is the possibility of growing quite large, high-quality single crystals from solution, thus making it very suitable for experimental studies. Indeed, a large wealth of experimental data has been accumulated during the second half of the past century.^{1,2}

Phosphates in KDP are linked through approximately planar H-bonds forming a three-dimensional network. In the paraelectric (PE) phase at high temperature, the H-atoms occupy with equal probability two symmetrical positions along the H-bond separated a distance δ , which characterizes the so-called disordered phase. Below the

critical temperature $T_c \approx 122$ K, the protons localize into one of the symmetric sites, thus leading to the ordered FE phase. Here, the spontaneous polarization P_s appears perpendicular to the proton ordering plane, and the PO_4 tetrahedra distort. The proton configuration in this phase is depicted in Fig. 1; each PO_4 unit has two covalently bonded and two H-bonded hydrogen atoms, following Slater's ice rules⁸. The oxygen atoms that bind covalently to the hydrogen are called *acceptor* (O2 in Fig. 1), and those H-bonded are called *donors* (O1 in Fig. 1).

A striking feature common to all H-bonded ferroelectrics is undoubtedly the huge isotope effect observed upon deuteration. In fact, the deuterated compound (DKDP) exhibits a T_c about two times larger than KDP. This giant effect was first explained by the quantum tunneling model proposed in the early sixties⁹. Within the assumption of interacting, single-proton double wells, this model proposes that individual protons tunnel between the two wells. Protons are more delocalized than deuterons, thus favoring the onset of the disordered PE phase at a lower T_c . Improvements of the above model include coupling between the proton and the K- PO_4 dynamics.^{10–13} These models have been validated *a posteriori* on the basis of their predictions, although there is no direct experimental evidence of tunneling. Only very recent neutron Compton scattering experiments seem to indicate the presence of tunneling¹⁴. However, the connection between tunneling and isotope effect remains unclear, in spite of recent careful experiments.¹⁵

On the contrary, a series of experiments carried out since the late eighties^{16–20} provided increasing experi-

mental evidence that the geometrical modification of the hydrogen bonds and the lattice parameters upon deuteration (Ubbelohde effect²¹) is intimately connected to the mechanism of the phase transition. The distance δ between the two collective equilibrium positions of the protons (see Fig. 1) was shown to be remarkably correlated with T_c .¹⁹ Actually, it seems that proton and host cage are connected in a non-trivial way, and are not separable.²² These findings stimulated new theoretical work where virtually the same phenomenology could be explained without invoking tunneling.^{23–25} However, these theories were developed at a rather phenomenological level. Only very recently, the first *ab initio* calculations, based on Density Functional Theory (DFT), were conducted in these systems.^{26–30} These approaches have the advantage of allowing for a confident and parameter-free analysis of the microscopic changes affecting the different phases in this system.

In this work we investigate, using DFT electronic structure calculations within the generalized gradient approximation to exchange and correlation, the relationship between proton ordering, internal geometry, polarization, tunneling and isotope effects in KDP (details of the methods used are exposed in Section II). To this end, consideration of the following questions naturally arises: (1) What is the microscopic mechanism which gives rise to the FE instability?, (2) How do local instabilities lead to the double-site distribution in the PE phase?, (3) What is the quantum origin of the geometrical effect?, (4) What is the main cause of the giant isotope effect: tunneling or the geometrical modification of the H-bonds?, (5) How does pressure affect the energetics and the structural parameters in the system?

With the aim of shedding light on the above formulated questions, and on the general problematic in KDP, we conducted different computational experiments and made a revision of previously obtained results. First, we carried out electronic structure calculations in the tetragonal unpolarized phase (PE), forcing protons to be in the middle of the O-H-O bonds. Calculations in the polarized phase (FE), with the H ordered off-center, were performed in both, the tetragonal fixed cell and in the completely relaxed cell, which is orthorhombic. We studied the structures and the charge reorganization leading to the FE instability. These results are presented in Section III. In Section IV, we analyze global instabilities in KDP to understand the relation between proton ordering and polarization. To address the tunneling issue, we studied local instabilities by determining the dependence of the system energetics upon the proton position in the H-bonds under various conditions: allowing or not K and P ions relaxations, and considering also individual proton and small cluster displacements. Besides, we show in this section a calculation of the momentum distribution of the proton along the H-bond in different phases and compare the results with recent experimental data. Section V is devoted to a thorough study of quantum fluctuations, and the controversial problem of the isotope effects. We

show how a self-consistent quantum modeling, based on our first principles calculations, is able to explain the striking mass dependence of the geometrical effect. In Section VI, we present calculations of the energetics and the structural parameters as a function of pressure. We show that the results of related experiments under pressure are explained by the non-linear relationship between deuteration and geometric effects, derived in the previous section. Finally, in Section VII we discuss the above issues, and elaborate our conclusions.

II. AB INITIO METHODS

We have performed *ab initio* calculations of KDP, within the framework of DFT,^{31,32} using two different pseudopotential codes, one based on localized basis sets (LB), and another using plane waves (PW).

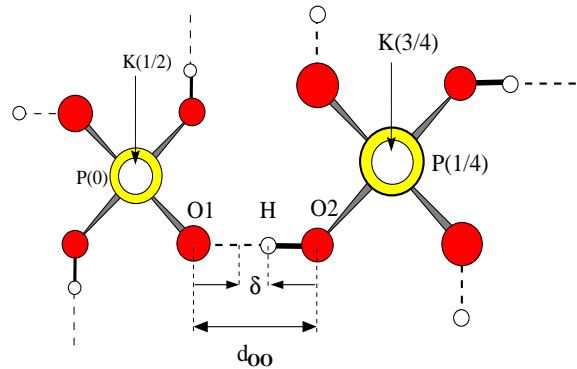


FIG. 1. Schematic view of the internal structure of KDP along the tetragonal axis. The fractional coordinates of P and K atoms along the c axis, are indicated in brackets. Covalent and H-bonded hydrogens are connected to corresponding oxygens by full and broken lines, respectively.

The LB calculations were carried out using the SIESTA program.^{33,34} This is a fully self-consistent DFT method that employs a linear combination of pseudoatomic orbitals (LCAO) of the Sankey-Niklewsky type as basis functions³⁵. These basis functions are strictly confined in real space, what is achieved by imposing in the pseudoatomic problem (i.e. the atomic problem where the Coulomb potential has been replaced by the same pseudopotential that will be used in the solid state), the boundary condition that the orbitals vanish at a finite cutoff radius, rather than at infinity as for the free atom. Therefore, these solutions are slightly different from the free atom case, and have somewhat larger associated energies because of the confining potential. The relevant parameter for this approximation is precisely the orbital confinement energy E_c , given by the energy difference between the eigenvalues of the confined and the free orbitals. In our calculations, we used a value of $E_c = 50\text{meV}$. By decreasing this value further, we checked that we obtain total energies and geometries with sufficient accuracy. For the representation of the valence

TABLE I. Comparison of the ab-initio (LB and PW) internal structure parameters with DKDP experimental data⁴¹ for the different cases considered in the text. The notation is the same used in the experimental works referred. γ is the relative z-displacement of the K and P atoms from the equidistant situation (see definition in section IV.A). Distances in Å and angles in degrees.

Structural parameters	Tetragonal					Orthorhombic		
	Unpolarized (UT)			Polarized (PT)		LB	PW	Exp.
	LB	PW	Exp. (234 K)	LB	PW			
d(P-O2)	1.594	1.565	1.543	1.624	1.599	1.625	1.593	1.578
d(P-O1)	1.594	1.565	1.543	1.571	1.536	1.569	1.528	1.509
d _{OO}	2.422	2.418	2.522	2.465	2.497	2.480	2.491	2.533
δ	0	0	0.443	0.275	0.371	0.310	0.381	0.472
γ	0	0	0	0.072	0.107	0.082	0.120	0.130
< O2-P-O2	111.2	110.6	110.5	106.4	106.2	105.6	106.3	105.7
< O1-P-O1	111.2	110.6	110.5	114.5	115.3	115.1	115.8	115.7
<O1...H-O2	177.4	178.3	177.1	177.0	178.9	177.3	178.9	179.8
θ	60.2	59.4	61.6	61.7	61.6	62.8	62.0	62.3
E _{gap} (eV)	5.64	5.78		5.55	5.65	5.52	5.65	

electrons in the LB method we used double-zeta bases with polarization functions (DZP). This means two sets of orbitals for the angular momenta occupied in the isolated atom, and one set of orbitals for the first non-occupied angular momentum (polarization orbitals). Again, this size of the basis set turns out to be accurate enough for our purposes.

The exchange-correlation energy terms were computed using the Perdew-Burke-Ernzerhof (PBE) form of the generalized gradient approximation³⁶. This type of functionals has already been used to describe hydrogen-bonded systems, with quite good accuracy.³⁷ We also tried the BLYP functional³⁸, which gives very good results for molecular systems. However, the results in the solid state were of quality inferior than PBE. We used non-local, norm-conserving Troullier-Martins pseudopotentials³⁹ to eliminate the core electrons from the description. We also included nonlinear core corrections (NLCC) for a proper description of the K ion, due to an important overlap of the core charge with the valence charge density in this atom. We checked this approximation by comparing with a K⁺ pseudopotential that includes the 3s and 3p shells explicitly in the valence, as semicore states (9 explicit electrons per K atom). The semicore results are very closely reproduced by the core-corrected calculations. For the real-space grid used to compute numerically the Coulomb and exchange-correlation integrals^{33,34}, we used an equivalent energy cutoff of 125 Ry.

The pseudopotential PW calculations were carried out with the PWSCF code⁴⁰, with the same exchange-correlation functional and pseudopotentials, except for the core-corrected K, where we used a semicore pseudopotential for K⁺ (9 electrons per K atom). The plane wave expansion was cut off at a maximum PW kinetic energy of 150 Ry. Such a high cutoff was necessary to

obtain convergence in the internal degrees of freedom, particularly the hydrogen-bonded units. The PWSCF code also allows for the computation, within the linear response regime, of vibrational and dielectric properties such as phonon frequencies, Born effective charges and dielectric constant. Phonon eigenvectors were used to calculate the total energy curves under pressure, by constraining the optimization to motions preserving the pattern of the ferroelectric normal mode, which is related to the parameter δ .

The PE phase of KDP has a body-centered tetragonal (*bct*) structure with 2 formula units per lattice site (16 atoms). For the LB calculations that describe homogeneous distortions, we used the conventional *bct* cell (4 formula units), but doubled along the tetragonal *c* axis. This supercell comprises 8 formula units (64 atoms). A larger supercell is required to describe local distortions. To this end, we used the equivalent conventional *fcc* cell (containing 8 formula units, and axes rotated through 45 degrees with respect to the conventional *bct* cell), also doubled along the *c*-axis (128 atoms). The LB calculations were conducted using a Γ -point sampling of the Brillouin zone (BZ). This choice of sampling proved sufficient provided the large supercells used in the calculations.

Most of the calculations have been done using the LB approach which, within the approximations described above, turned out into quite a fast computational procedure, compared to PW calculations. As a test, we checked the LB approach against the PW results. The PW calculations were carried out on the 16-atom *bct* unit cell, with a BZ sampling consisting of 8 centered Monkhorst-Pack k-points. This number of points was checked for convergence, and proved sufficient. The results for the geometrical parameters are reported in table I. It can be seen that the LB values are of quality

comparable to the PW results. The differences can be attributed mainly to the approximation made with the confinement of the orbitals in the LB calculations.

III. CHARACTERIZATION OF THE STRUCTURES AND CHARGE FLOW MECHANISMS

We first optimized the structure with paraelectric phase symmetry. To this end, we constrained the H-atoms to remain centered in the O-H-O bonds, and fixed the lattice parameters to the experimental values of the deuterated compound (DKDP) at $T_c + 5$ K ($a = b = 7.459$ Å and $c = 6.957$ Å) in the conventional *bct* cell.⁴¹ The choice of DKDP instead of KDP for the comparison with experiment is based on the fact that nuclear quantum effects, which are neglected in the first-principles calculations, are less important. Optimization of all the atomic positions leads to what we call the *unpolarized tetragonal* (UT) structure. This can be interpreted as an average of the true paraelectric phase. In fact, according to experimental data, in this latter the H-atoms are observed with equal probability in two symmetric off-centered positions along the H-bonds. In Table I we compare the relevant structural parameters resulting from both types of calculations and also experimental data. The agreement between the two theoretical approaches is quite good – thus validating the later use of the LB approach –, and their comparison with experiment is very satisfactory, except for the O-O distance d_{OO} which, specially in the UT case, turns out to be too short.²⁶ This delicate issue will be discussed below.

Maintaining the lattice parameters and constraining the K and P atoms to their centered positions in the UT structure, we next allowed for H off-center relaxation towards the ordered configuration sketched in Fig. 1. The O-O distance is also optimized. In this way we obtained a H off-center shift $\delta/2 = 0.154$ Å and an O-O distance of 2.472 Å. We will show below in more detail that the H off-centering produces an electronic charge redistribution from the neighborhood of the O2 atoms towards that of the O1 atoms. As a consequence, unbalanced forces are generated that favor pairing of the K and P atoms along the z axis, on the charge-excess side (O1) of the PO_4 units. The former observation indicates that, constraining the K and P to their centered positions, does not prevent the H atoms from abandoning the center of the H-bonds. The centered position for the H atoms is always unstable, as we will show in the next Section.

The next step was to relax also the positions of the K and P atoms, thus leading to the *polarized tetragonal* (PT) structure, whose geometrical parameters are listed in Table I. This PT structure is not yet the ground state, because the ferroelectric distortion is coupled to a shear strain mode. It is this acoustic mode that becomes soft before the FE mode, thus piloting a structural transition to an orthorhombic phase, which is very similar

to the PT. This coupling can be observed in the σ_{xy} , off-diagonal components of the calculated stress tensor. According to this observation, we relaxed again all the internal degrees of freedom, but now fixing the simulation cell to the experimental orthorhombic structure of DKDP at $T_c - 10$ K. This corresponds to lattice parameters $a = 10.598$ Å, $b = 10.496$ Å and $c = 6.961$ Å in the conventional *fcc* cell.⁴¹ The calculated geometrical parameters, which are close to those of the PT structure, are shown in the last three columns in Table I compared to experimental data.

In the experimental orthorhombic structure, however, the stress tensor is diagonal but not isotropic. This indicates that, if the lattice parameters were also to be optimized, the b/a ratio would be different from the experimental value. In addition, the isotropic part of the stress (the pressure) is non-zero, thus indicating a small difference in equilibrium volume between calculations and experiment. In general the agreement is quite reasonable, again with the exception of the O-O distance, which is 0.1 Å too small in the UT structure. This is a very important issue, because the potential for the deuterons (or protons) in the H-bond is extremely sensitive to the O-O distance⁴². In the present DFT-PBE calculations for the UT structure this distance is 2.42 Å, i.e. 0.1 Å shorter than the experimental value⁴¹. This difference, which can even change the shape of the potential felt by the deuteron in the H-bond, cannot be fully attributed to the optimization for centered deuterons. In fact, it persists when we optimize the structure in the orthorhombic FE phase, although slightly reduced (2.49 Å vs. 2.53 Å). One possible reason are quantum nuclear effects. Our calculations are for clamped nuclei, corresponding to infinite deuteron mass. If quantum dynamics of deuterons was to be included, it would slightly increment this discrepancy because nuclear delocalization favors shorter H-bonds. This can also be seen from the fact that the experimental O-O distance for protons is shorter than for deuterons (Ubbelohde effect). Therefore, the inclusion of quantum effects would imply even shorter O-O distances. It is neither a problem of the pseudopotential approach, which has been tested against all-electron calculations.

We conclude, then, that the main origin of the underestimation of the O-O bond length is in the approximate character of the exchange-correlation functional. In fact, calculations for related gas-phase systems like H_3O_2^- indicate a similar 0.06 Å underestimation when comparing GGA values to correlated quantum chemical calculations⁴³. Moreover, present test calculations for the water dimer also indicate an underestimation of the d_{OO} distance by 0.06 Å with respect to experimental values⁴⁴.

Therefore, the differences in the H-bond geometry app-

TABLE II. Changes $q(\text{PT}) - q(\text{UT})$ in the Mulliken orbital and bond overlap populations in going from the UT to the PT configuration, in units of $e/1000$.

O1	O2	P	K	H	O1...H	O1-P	O2-H	O2-P
+82	-58	-8	-3	-17	-91	46	70	-44

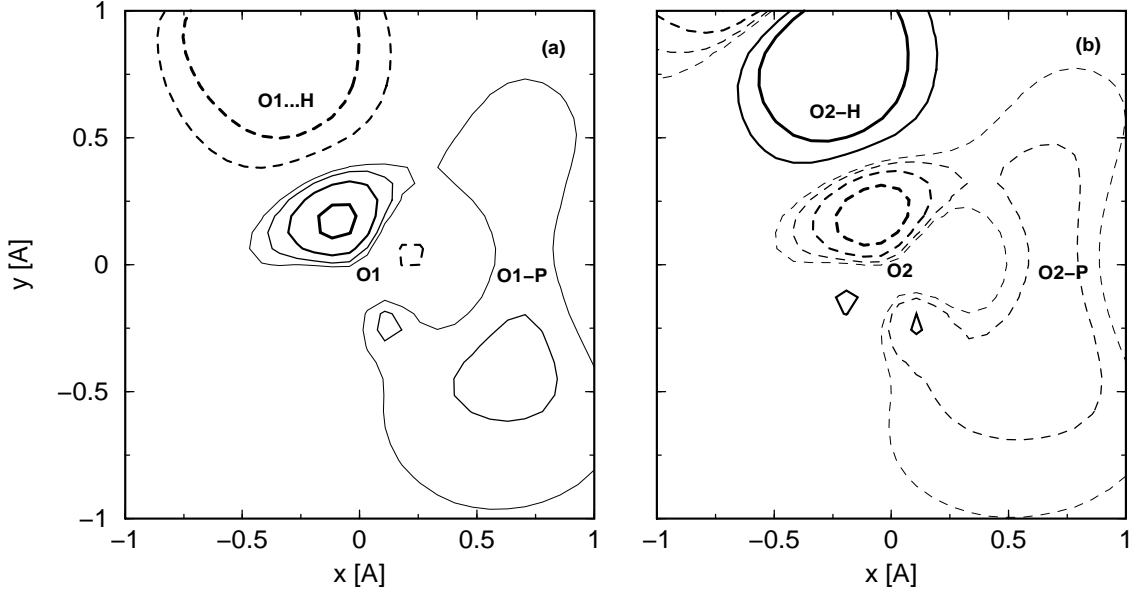


FIG. 2. Differential charge density contours $\Delta\rho(\mathbf{r})$ in the planes containing the following atoms: (a) P-O1...H, (b) P-O2-H. Labels O1 and O2 denote the positions of the respective nuclei, positioned at (0,0). Labels O2-P and O1-P indicate the position of the center of the corresponding bonds. The same convention is used for the O2-H and O1...H bonds. Positive (negative) contours are in solid (dashed) lines. The thickest lines represent an absolute value of $2.96 \times 10^{-3} \text{ e}\text{\AA}^{-3}$. The thinner lines are obtained by successively halving this value, down to $3.70 \times 10^{-4} \text{ e}\text{\AA}^{-3}$.

ear to be mainly due to the approximate character of the exchange-correlation term. Unfortunately, at present, a sufficiently well validated and efficient scheme to go beyond GGA is lacking. Therefore, in order to avoid problems derived from this feature in the study of the stability of local cluster distortions in next Section, we decided to fix the O-O distances in the host to the experimental values.

With the purpose of analyzing the charge redistributions produced by the ordered proton off-centering, we computed the changes in the Mulliken orbital and bond-overlap populations in going from the UT to the PT configuration, as shown on Table II. Mulliken populations depend strongly on the choice of the basis set. Differences, however, are much less sensitive.

An increase of the charge localized around O1 can be clearly observed; the main contribution ($\approx 70\%$) is provided by a decrease in the O2 charge.²⁶ The trends observed in Table II are confirmed by the charge density difference $\Delta\rho(\mathbf{r}) = \rho_{PT}(\mathbf{r}) - \rho_{UT}(\mathbf{r})$. In Fig. 2a and 2b we plot cuts of the above quantity in the planes determined by the atoms P-O1...H and P-O2-H, respectively. A combined analysis of both, Table II and Fig. 2a, in-

dicates a significant enhancement of the population of the O1 atom, accompanied by a smaller increment in the O1-P orbitals. This happens at the expenses of the population of the O1...H and O2-P overlap orbitals, and the population of the O2 atom. Therefore, as two H-atoms move away from O1 and other two approach O2, the O1-H bond weakens and the O2-H bond strengthens. The charge localizes mostly around O1 and, to a lesser extent, in the P-O1 orbitals. This is consistent with the increase of $d(\text{O1} - \text{O2})$ and the decrease of $d(\text{P} - \text{O1})$ reported in Table I. The contrary occurs in the vicinity of the O2 atom, as indicated by the orbital and bond-overlap populations in Table II and the contours in Fig. 2b. The overall effect is a flow of electronic charge from the O2 side of the tetrahedron towards the O1 side, and a concomitant modification of its internal geometry. The charge redistribution is rather local, and gives rise to a polarization composed by electronic and ionic contributions⁴⁵. This polarization, whose origin can therefore be traced back to the off-centering of the H-atoms in the perpendicular plane, is intimately linked to ferroelectricity. In fact, the combined motion of all the atoms and the concomitant electronic redistribution corresponds to

an unstable phonon in the UT structure⁴⁶. When this phonon mode freezes into one of the two stable minima, we obtain the PT structure which has a polarization, and is thus ferroelectric. A schematic view of this combined effect is presented in Fig. 3.

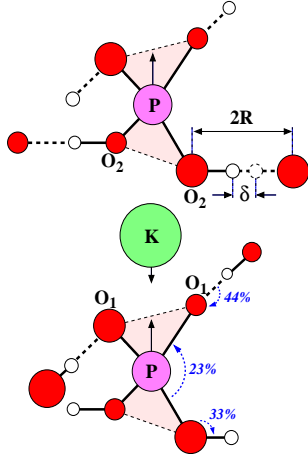


FIG. 3. Schematic view, perpendicular to the c -axis, of the atomic motions (solid arrows) and electronic charge redistributions (dotted curved arrows), happening upon off-centering of the H-atoms. The percentages of the total charge redistributed are also shown for the charge-transfers occurring between different orbitals and atoms.

A further confirmation of these ideas comes from the saturated polarization which was obtained from linear response calculations of Born effective charges.^{46,40} Considering the eigenvector of the FE mode $e_\alpha(i)$, where α indicates the Cartesian coordinate and i the ion, we calculated the dynamical effective charge in the z direction:

$$Z_z^*(FE) = \sum_i \sum_\alpha Z_{z\alpha}^*(i) \frac{e_\alpha(i)}{\sqrt{m_i}} = 1.6 e. \quad (1)$$

The effective charge components in the x and y directions vanish. $Z_z^*(FE)$ is multiplied by the FE-mode amplitude corresponding to the stable minimum, giving rise to a saturation polarization of $P_s = 3.25 \mu\text{C}/\text{cm}^2$, slightly lower than experimental values. Analyzing the individual contributions, we observe that a substantial part arises, in fact, from the P ions. However, this contribution is only a 40% of the total polarization. The other 60% arises from the H atoms through a non-diagonal xz (or yz) component of the effective charge tensor. This component is $Z_{xz}^*(H) = 0.6 e$ while $Z_{zz}^*(P) = 3 e$, but the displacement of the H atoms in the x (or y) axis is more than five times larger than that of the P ions along the z axis. This, and the fact that there are twice as many H than P in the unit cell, explains why H contributes as much as P to the polarization. The interesting observation is that the H atoms move in the plane perpendicular to the z axis. Therefore, their off-diagonal contribution can only be due to electronic polarization effects. Although

the effective charges of the K and O atoms are not null, their small displacements lead to negligible contributions to the spontaneous polarization.

IV. GLOBAL AND LOCAL FERROELECTRIC INSTABILITIES

A. Correlation Between Proton Ordering and Polarization

In the previous section we showed that there is an instability of the system towards the PT structure as hydrogens collectively move away from the centers of the O-H-O bond. From our simulations, we observe that when the protons are constrained to remain centered in the H-bonds, the K and P atoms are stable in their centered positions. However, centering the heavy atoms does not imply the centering of the H-atoms. Protons, in fact, are never stable at their centered positions. This provides a strong evidence that the origin of ferroelectricity is in the off-center ordering of the protons, and that proton off-centering and ferroelectricity are very correlated phenomena.

To identify the driving mechanism of the ferroelectric instability, we analyzed the relationship between proton ordering and polarization. To this purpose, we investigated the *ab initio* potential energy surface (PES) as a function of the proton off-centering parameter $\delta = d_{OO} - 2d_{OH}$, and the K-P relative displacement along the c -axis, which we quantify in terms of the parameter $\gamma = d_{PP} - 2d_{KP}$, with d_{KP} the smallest K-P distance. It is worth mentioning here that γ is a measure of polarization, since a test calculation provided us a linear relationship between these quantities.

We fully relax the oxygen positions for each chosen (δ, γ) pair, and plot the energy contours of the bidimensional PES in the inset to Fig. 4. The characteristics of this PES are as follows: it exhibits a saddle point at $\delta = \gamma = 0$, and two equivalent minima at $(\delta, \gamma) \simeq \pm(0.3, 0.15) \text{ \AA}$. On the one hand, from the energy contours it can be seen that at $\delta = 0$ (centered protons) there is no instability for any value of γ , i.e. the crystal is stable against polarization ($\gamma \neq 0$) unless the protons are ordered off-center. On the other hand, even for vanishing γ (polarization) the energy minimum corresponds to a finite δ , i.e. protons are always collectively unstable at the H-bond center. This is further visualized in Fig. 4, where we plot the energy profiles as a function of δ for different fixed values of γ . For $\gamma = 0$, the energy profile exhibits a double-well in the δ coordinate with a barrier of $\simeq 6$ meV per molecular unit. For increasing values of γ the minima are always at $\delta \neq 0$, up to a value of $\gamma \approx 0.02 \text{ \AA}$, where one of the two minima completely disappears. Therefore, we conclude from the above considerations that the source of the ferroelectric instability is the H off-centering, and not viceversa.

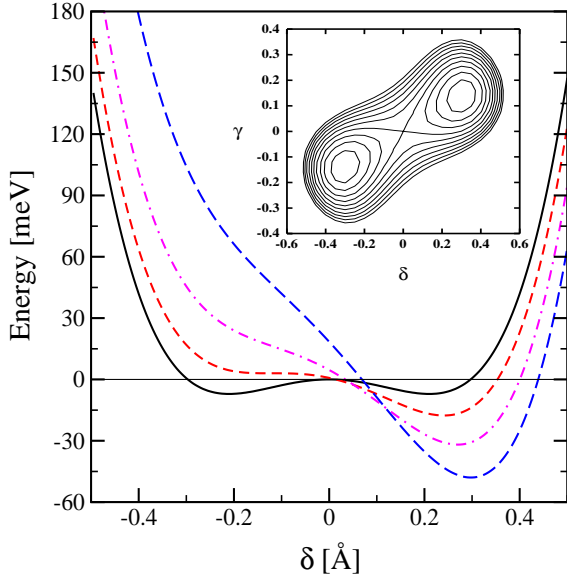


FIG. 4. Energy profiles as a function of δ , for values of $\gamma = 0$ (solid line), 0.02 (short-dashed), 0.05 (dot-dashed) and 0.1 (long-dashed) \AA . The inset shows equispaced energy contours (step = 13.6 meV/ KH_2PO_4 unit). The minima at $(\delta, \gamma) \simeq \pm(0.3, 0.15)\text{\AA}$ lie $\simeq 50$ meV below the saddle point at $(0,0)$

B. Local Instabilities, Quantization in Small Clusters, and the Nature of the Paraelectric Phase

We now address the microscopic origin of the observed proton double-occupancy in the PE phase⁴¹, which is an indication of the order-disorder character of the transition. This phenomenon can be ascribed either to static or thermally activated dynamic disorder, or to tunneling between the two sites. Any of these possibilities requires the search for instabilities with respect to correlated but localized H motions in the PE phase, including also the possibility of heavy-ions relaxation. In fact, correlated motions of a large number of protons become increasingly unlikely in a tunneling scenario, because this implies higher barriers and heavier effective masses, thus reducing the tunneling probability. To analyze localized distortions we consider increasingly larger clusters embedded in a host paraelectric matrix. For the reasons exposed in the previous Section, the host is modeled by protons centered between oxygens, and the experimental structural parameters (including the O-O distances) of KDP at $T_c^{KDP} + 5$ K (127 K).⁴¹ In order to assess the effect of the volume increase observed upon deuteration, we also analyze the analogous case of D in DKDP by expanding the host structural parameters to the corresponding experimental values at $T_c^{DKDP} + 5$ K (234 K).⁴¹

We analyze results for different clusters comprising N hydrogens (deuteriums): (a) N=1 H(D) atom, (b) N=4 H(D) atoms which connect a PO_4 group to the host,

(c) N=7 H(D) atoms localized around two PO_4 groups, and (d) N=10 H(D) atoms localized around three PO_4 groups. For all these clusters we consider correlated motions with the pattern shown in Fig. 1, which are the most favorable for exhibiting FE instabilities, as it was illustrated in the previous section. This correlated pattern, is represented by a single collective coordinate x whose value coincides with the H(D) off-center displacement $\delta/2$. Two cases are considered: (i) first, we allow for the motion of H atoms alone, maintaining all other atoms fixed, (ii) second, we also allow for the relaxation of the heavy ions K and P, which follow the ferroelectric mode pattern^{47,46}, as expected. Subsequent quantization of the cluster motion in the corresponding effective potential allows for the determination of the importance of tunneling in the disordered phase. Rigorously, the size dependence should be studied for larger clusters than those mentioned here. However, it will be shown below that short-range quantum fluctuations in the PE phase are sufficiently revealing, especially far away from the critical point.

In Fig. 5 we show, for the clusters considered, the total energy variation as a function of x . For the case of H motions alone, we do not observe any instability for N=1 and N=4, both in KDP and DKDP. A small barrier of ~ 6 meV appears in DKDP for the N=7 move, as shown in Fig. 5(b) (open squares). This barrier grows up to ≈ 25 meV for the N=10 cluster in DKDP (open circles).

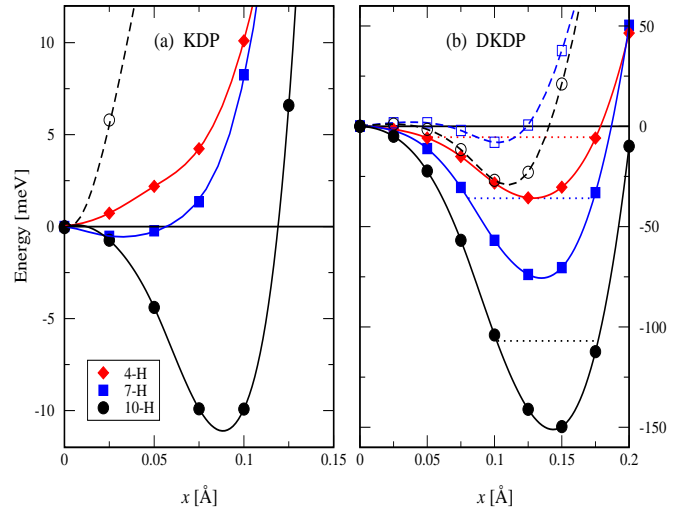


FIG. 5. Energy profiles for correlated local distortions in (a) KDP and (b) DKDP. Reported are clusters of: 4 H(D) (diamonds), 7 H(D) (squares), and 10 H(D) (circles). Empty symbols and dashed lines indicate that only the H(D) atoms move. Motions that involve also heavy atoms (P and K) are represented by filled symbols and solid lines. Lines are guide to the eye only.

However, quantum mechanical calculations of the cluster

levels, which will be described below, yield ground states (GS) quantized above the barriers and, consequently, the absence of tunneling in those cases (see Fig. 5). In KDP, even the largest cluster considered is very stable, as indicated by the open circles in Fig. 5(a). The result for KDP suggests to rule out this type of motions in the paraelectric phase, because they are incompatible with double site occupancy.

In a second step we considered also the motion of the heavy atoms in the above correlated local motions. The situation changed drastically, as shown by the solid lines and full symbols in Fig. 5(a) and (b). In fact, clusters involving two or more PO_4 units – cases (c) and (d) above – exhibit instabilities in both KDP and DKDP, with a significant barrier in DKDP for case (d), of the order of ≈ 150 meV. We note here that the instability appears in clusters which are sufficiently large, thus providing a measure of the FE correlation length. Moreover, the instabilities are much stronger (and the correlation length accordingly shorter) in the expanded DKDP lattice, than in KDP.

We treat these clusters quantum-mechanically, by solving the Schrödinger equation for the collective coordinate x . This is done for each cluster in the corresponding effective potentials of Fig. 5. The effective mass for the local collective motion of the cluster is calculated as $\mu = \sum_i m_i a_i^2$, where i runs over the displacing atoms and m_i are their corresponding atomic masses. a_i is the i -atom displacement at the minimum from their positions in the PE phase, relative to the H(D) displacement. The effective masses per H(D) calculated for these correlated motions in different clusters are about $\mu_H \approx 2.3$ ($\mu_D \approx 3.0$) proton masses (m_p) in KDP (DKDP), respectively. The calculation of the GS energy in the *heavy clusters*, leads now to quantized levels below the barriers, as shown by dotted lines in Fig. 5(b), for all clusters in DKDP. This is a clear sign for tunneling arising from correlated D motions involving also heavy ions. These collective motions can be understood as a local distortion reminiscent of the global FE mode.⁴⁶ In KDP, however, even the largest cluster considered ($N=10$), has the GS level quantized above the barrier. The onset of tunneling at a critical cluster size, provides a rough indication of the correlation volume: it comprises more than 10 hydrogens in KDP, but no more than 4 deuteriums in DKDP.⁴⁹ We clearly observe, then, that the dynamics of the order-disorder transition would involve fairly large H(D)-clusters together with heavy-atom (P and K) displacements. Thus, the observed proton double-occupancy is explained in our calculation by the tunneling of large and *heavy* clusters. The last conclusion is confirmed by the double-site distribution determined experimentally for the P atoms.^{50,51}

A possible scenario for the FE phase transition would then be the following: the PE phase is made of clusters of different size, some of them (the large ones) preserve the FE structure, i.e. do not exhibit double site H(D) occupancy because the barrier is too high. Other clus-

ters (smaller) have lower barriers and smaller effective masses, and thus can tunnel, giving rise to double occupancy. The effect of temperature is that of modifying the preferential cluster size, which grows as a measure of the correlation length on approaching the transition. When the average cluster size reaches a value in which neither tunneling nor thermal hopping are anymore allowed, then the phase transition takes place. Of course, this is a mean field vision, but we believe that the picture is quite plausible.

C. Momentum Distributions

Since Blinc's model proposal,⁹ it has been subject of controversy whether the protons are actually tunneling between the two equivalent sites along the bridges, or they are localized in one of these sites and jump to the other through phonon assisted tunneling in the paraelectric phase. Reiter et al.¹⁴ have recently attempted to elucidate this question by performing neutron Compton scattering experiments. Due to the much shorter time scale of this experiment, compared to typical times for phonon assisted jumps in the paraelectric phase, it is claimed that it is possible to distinguish between a proton coherently distributed between the two equivalent sites, and one which is alternatively occupying one site or the other. In this experiment, the momentum distribution along the bridge, $n(p)$, has been obtained by inverting the measured scattering function under plausible conditions.¹⁴ Very significant changes in $n(p)$ are observed when going through the transition, which were not to be expected if the proton was localized only in one of the equivalent sites, in both phases. As shown by the solid lines in Fig. 6, $n(p)$ is considerably narrower in the high temperature phase, indicating an increase in the spread of the region where the proton is coherently distributed (the wave packet). More conclusively, the high temperature distribution shows a zero and a subsequent oscillation which correspond precisely to a double peaked spatial wavefunction, i.e. the proton coherently distributed over both sites along the bond. In contrast, well below T_c , $n(p)$ shows a single and broader maximum at $p = 0$, thus indicating single-site occupancy.

Our calculations for the coherent motion of hydrogen clusters with fixed heavy ions, in a host of a mean paraelectric phase, indicate that only very large clusters would exhibit double well potentials with energy barriers high enough to allow for collective tunneling. On the other hand, considerably smaller clusters are able to tunnel if also the heavy ions are allowed to move coherently with H in KDP, or with D in DKDP. Therefore, Compton scattering results can be explained if the observed coherent double peaked distribution of a proton along a bridge is interpreted as part of a coherent motion together with heavy ions in a cluster.

Since the largest cluster we treated in KDP is not able

to tunnel, a direct comparison of our momentum distribution calculations in the PE phase with experiment is not feasible. Instead, we can make a prediction of what would the $n(p)$ distribution be like, in the PE phase of DKDP. For this purpose, we considered the corresponding double-well potentials as functions of the position of D along the bridge, for the 4-D and 7-D clusters in DKDP. We calculated the wavefunctions with the cluster effective masses $\mu = 10.4 m_p$ and $21.4 m_p$, respectively. The resulting momentum distributions of DKDP in the PE phase are shown in Fig. 6 (right panel), together with the experimental curve of KDP for illustrative purposes. The second oscillation arises from the quantum coherence of the real space distribution. As the effective mass of the cluster increases, the second oscillation has larger amplitudes, while the main oscillation remains unchanged.

In the ferroelectric phase of KDP the proton distribution is single peaked, corresponding to a single-well anharmonic potential for each proton. The momentum distribution calculated for a single proton wave function in such potential is shown by the dashed line in the left panel of Fig. 6. In order to understand the difference with the experimental data, we performed another calculation where the surrounding ions are allowed to relax. This leads to a shallower potential, but the effective mass also increases. The result, shown as a dotted line, deviates even more from the data. The deviation from experiment, observed for the uncorrelated proton distribution (dashed line), may be due to the broadening effect of temperature on the distribution of the host ions. It is worth mentioning that differences between results from the present calculations and previous preliminary ones²⁷ are due to refinements of the potentials performed presently.

V. QUANTUM DELOCALIZATION AND THE GEOMETRICAL EFFECT

A. Geometrical Effect vs. Tunneling

We now address the origin of the huge isotope effect on T_c observed in KDP and also in the isomorphous H-bonded crystals in the family. For forty years, starting from the pioneering work of Blinc,⁹ the central issue in KDP has been whether tunneling is or not at the root of the large isotope effect, a fact that was never rigorously confirmed. Moreover, a crucial set of experiments pointing against the tunneling picture was recently conducted by Nemes and co-workers: by applying pressure, they conveniently tuned the D-shift parameter δ_{DKDP} in DKDP to make it coincide with the H-shift parameter δ_{KDP} in KDP, and they observed that T_c^{DKDP} almost coincided with T_c^{KDP} , in spite of the mass difference between D and H in both systems.^{18,19,52} This suggests that the modification of the H-bond geometry by deuteration – the *geometrical*

effect – is a central mechanism in the transition, and is intimately connected with the isotope effect.

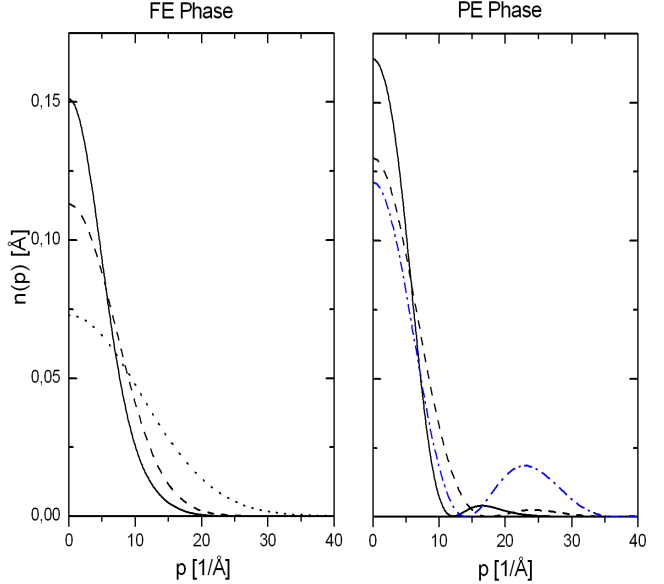


FIG. 6. Momentum distributions along the H-bond in both phases of KDP. Experimental data are shown in solid lines.¹⁴ Left panel (FE phase): calculations for single uncorrelated H motion (dashed line), and for H correlated with host relaxation (dotted line). Right panel (PE phase): calculations for 4-D and 7-D cluster dynamics, as explained in text (dashed and dot-dashed lines, respectively).

As the cluster size grows ($N \rightarrow \infty$), the tunnel splitting Ω vanishes. However, only large clusters are expected to be relevant for the nearly second-order FE transition in these systems.⁵⁶ Thus, for large tunneling clusters the potential barrier is sufficiently large, and the GS levels are deep enough (see Fig. 5) that the relation $\hbar\Omega_{H(D)} \ll K_B T_c$ is satisfied, so much for D as for H. Therefore, according to the tunneling model, the above relation implies that a simple change of mass upon deuteration at fixed potential cannot explain the near duplication of T_c . In fact, if we consider the largest cluster ($N=10$) in Fig. 5 for DKDP, which is larger than the crossover length in this system, we have that the GS level for the deuterated case (calculated with an effective mass of $10\mu_D = 35.4 m_p$) is around $E_{GS} = -107$ meV, well below the central barrier, and the tunnel splitting amounts to $\hbar\Omega_D = 0.34$ K. Modifying the mass at fixed potential ($10\mu_H = 25.3 m_p$) leads to a tunnel splitting of $\hbar\Omega_D = 1.74$ K. Since $T_c^{DKDP} \approx 229$ K, the relation $\hbar\Omega_{H(D)} \ll K_B T_c$ clearly holds, and the change in Ω at fixed potential accounts only for a small change in T_c . This is in agreement with the high-pressure experiments mentioned above,^{18,19,52} where at fixed structural conditions, the isotope effect in T_c appears to be rather modest.

Also the geometric effect in the H-bond is very small

at fixed potential. In fact, the proton and deuteron wave functions (WF) in the DKDP potential for the N=7 cluster, which are reported in Fig. 7 (a), are only slightly different. As a matter of fact, the distance between peaks as a function of the effective mass at fixed potential remains almost unchanged, as can be seen by the square symbols in Fig. 7 (c).

In contrast, the proton WF for the N=7 cluster in the KDP potential exhibits a single broad peak, as shown in Fig. 7 (a). But, how can we then explain such a large geometric change in going from DKDP to KDP? The first observation arises from what is apparent in Figure 5: energy barriers in DKDP are much larger than those in KDP, implying that quantum effects are significantly reduced in the expanded DKDP lattice. In fact, the proton WF in the DKDP potential has more weight in the middle of the H-bond ($x \approx 0$) than the deuteron WF (Fig. 7 (a)). That is, due to zero-point motion, protons are more favored in the H-centered position than deuterons. This affects the covalency of the bond, which becomes stronger as the proton moves to the H-bond center, as discussed in Section III. The geometric change of the O-H-O bridge, produced by the combined effect of quantum delocalization and gain in covalency, affects in turn the crystal cohesion. Thus, the increased probability of the proton to be midway between oxygens strengthens the O-H-O covalent grip and pulls the oxygen atoms together, causing a small contraction of the lattice. As will be shown in the following Section, this contraction has the effect of decreasing the barrier height, thus making the proton even more delocalized. This triggers a further contraction of the lattice, and so on in a self-consistent way. This self-consistent procedure is finally identified as the phenomenon that makes the lattice shrink from the larger classical value to the smaller value found for KDP. This phenomenon, triggered by tunneling and quantum delocalization, leads to an enhancement of the geometrical effect. The overall self-consistent effect is eventually much larger than the deuteration effect obtained at fixed potential, i.e. at fixed lattice constant.

To estimate an upper limit to that effect, we compared the lattice parameters and the bridge lengths by carrying out electronic calculations with classical nuclei (clamped nuclei). This was done for two different situations: one with the hydrogens forced to stay in the middle of the H-bond, and the other with the hydrogens fully off-centered in the FE state of KDP. In the latest case, the distance between oxygens is $d_{OO} \approx 2.50$ Å, falling to $d_{OO} \approx 2.42$ Å when H is centered. In addition, the lattice volume is contracted by about 2.3 %. Thus, the proton centering acts as a very strong attraction center, pulling the two oxygens together. We estimate that, at the equilibrium volume, the proton centering creates an equivalent pressure of ≈ 20 Kbar. In the true high-temperature PE phase, though, the protons are not centered in the middle of the H-bonds, but they are equally distributed on both sides of the bond, thus reducing the magnitude of the effect.

B. The Isotope Effect: a Nonlinear Self-consistent Phenomenon

In the previous subsection we discussed how a self-consistent mechanism combining quantum delocalization, the modification of the covalency in the bond, and the effect on the lattice parameters, can account for the large geometric effect observed upon deuteration. This mechanism is now capable of explaining, at least qualitatively, the increase in the order parameter and T_c with deuteration. This self-consistent mechanism has obviously its origin in the difference in tunneling induced by different masses, but is largely amplified through the geometric modification of bond lengths and energy scales.

To demonstrate the effect of isotopic substitution via this self-consistent non-linear mechanism, we constructed the following simple model: we considered the Schrödinger equation for the clusters with a WF-dependent term added to the bare potential. The effective potential reads:

$$V_{\text{eff}}(x) = V_0(x) - k|\Psi(x)|^2, \quad (2)$$

where x is the collective coordinate of the cluster and $V_0(x)$ is a quartic double-well similar to those of Fig. 5. The term in $|\Psi(x)|^2$ serves as a non-linear feedback in the model: when the particle is more delocalized, it has more weight in the middle of the H-bond. Then, $|\Psi(x)|^2$ increases at the center, the effective barrier is lowered, the particle further delocalizes, and so on, self-consistently. The bare potential can be written as

$$V_0(x) = E_b^0 \left[-2 \left(\frac{2x}{\delta_{\min}^0} \right)^2 + \left(\frac{2x}{\delta_{\min}^0} \right)^4 \right], \quad (3)$$

in terms of its energy barrier E_b^0 and minima separation δ_{\min}^0 . The parameters values $k = 20.2$ meV.Å, $E_b^0 = 35$ meV and $\delta_{\min}^0 = 0.24$ Å were chosen so as to qualitatively reproduce the WF profiles in the cases of KDP (broad single peak) and DKDP (double peak), for the same cluster size. Once these parameters are fixed, the WF self-consistent solutions depend only on the effective mass. Figure 7(b) shows the WF corresponding to μ_D (solid line) and μ_H (dashed line), which are similar to those calculated from the ab initio potentials for the N=7 cluster (Fig. 7(a)).

In Fig. 7(c), we show the distance between peaks δ_p in the WF as a function of the cluster effective mass μ . Starting from the finite value for μ_D (DKDP), δ_p decreases remarkably towards lower μ values, until it vanishes near μ_H (KDP) (see circles in Fig. 7(c)). This strong dependence of δ_p on the mass is in striking contrast with the very weak dependence obtained at fixed DKDP potential and geometry (square symbols). Such a large mass dependence, can now explain the large isotope effect found in KDP, via an amplified and self-consistent geometrical modification of the H-bond.

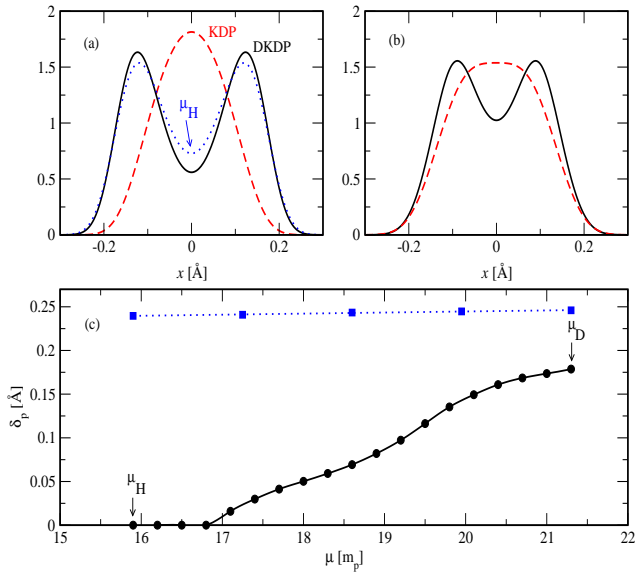


FIG. 7. WF in the 7-H(D) cluster PES for (a) *ab initio* and (b) self-consistent model calculations. Solid (dashed) lines are for D (H). Dotted line is for H in the DKDP PES. (c) WF peak separation δ_p as a function of the cluster effective mass μ (given in units of the proton mass) for the self-consistent model (circles) and for fixed DKDP potential (squares). Lines are guides to the eye.

VI. PRESSURE EFFECTS

Experiments under pressure carried out during the late eighties showed, within error bars, that T_c depends linearly on δ for different H-bonded ferroelectric materials.⁵² Strictly speaking, the linear relation is verified for some of these compounds within a restricted region of the T_c vs. δ plot. In the case of KDP, the linear behaviour appears to extend up to a pressure of 17 Kbar, where T_c vanishes. The need for very high pressures (≈ 60 Kbar) to achieve a vanishing T_c for DKDP and other related H-bonded compounds, precluded the generalization of the enunciated hypothesis, and motivated the development of improved diamond anvil cells. Nevertheless, a striking observation arises when the extrapolation of the linear behaviour in the mentioned materials is carried down towards lower values of T_c : the critical temperature appears to vanish for all systems, deuterated and protonated, with one, two and three-dimensional H-bond networks, around a seemingly universal point where $\delta = \delta_c \approx 0.2$ Å.⁵²

In particular, the effect of deuteration can be reverted by applying pressure, and the critical temperature of KDP can be reproduced by compressing DKDP in such a way that the structural parameter δ_{DKDP} assumes a value very close to that measured in KDP at the initial pressure.⁵² This is valid at all the measured pressures.

In this Section we explore the connection between pressure and isotope effect by means of first-principles cal-

culations and the aid of the previously introduced self-consistent model for the geometrical effect.⁵³ To this purpose, we first focus on first-principles calculations, where we used the PW approach explained in section II, combining ultra-soft (O and H) and norm-conserving (K and P) pseudopotentials.^{54,39} Using linear-response theory,⁴⁰ the unstable ferroelectric mode at the zone-centre was identified. This corresponds mostly to H-atoms displacements with the pattern shown in Fig. 3, with heavy ions displacing to a lesser extent. The O-atoms are practically fixed in this mode.

The FE mode amplitude is identified with the H off-centering coordinate (x). The total energy profile as a function of x displays an effective double-well potential for the FE mode.⁴⁶ Thus, the potential can be characterized by two parameters: the energy barrier E_b between the stable and the unstable ($x = 0$) configurations, and the separation between minima δ_m . The values of E_b vs. δ_m obtained under different applied pressures are plotted in Fig. 8. A nearly quadratic behaviour with simultaneous vanishing of E_b and δ_m is observed. Classically, ferroelectricity would disappear above ≈ 100 Kbar. However, the critical temperatures vanish at substantially lower critical pressures P_c , which are isotope-dependent: 17 Kbar for KDP and 60 Kbar for DKDP.⁵⁵ This can be understood by considering the quantum character of the nuclear dynamics. In fact, the zero-point energy, which is larger for the proton, should lower the effective energy barrier leading to lower critical pressures.

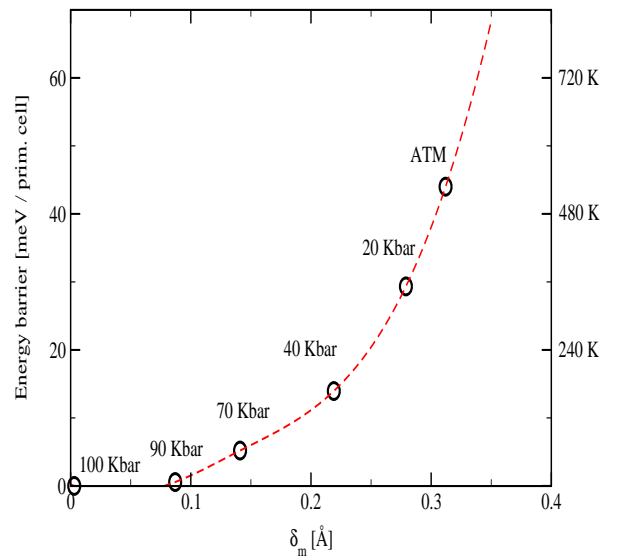


FIG. 8. Energy Barrier E_b as a function of the distance between the two minima of the double-well, δ_m , for different pressures. The dashed line is a guide to the eye. An approximate conversion to temperatures has been included to the right of the graph.

In Fig. 9 we show the two parameters of the double-well, i.e. E_b and δ_m , as a function of pressure. In this figure, critical pressures for KDP and DKDP are indicated by vertical arrows. These correspond, in our calculation, to different *classical* values of the minima separation δ_m , which are around 0.3 Å in KDP and 0.18 Å in DKDP. Experiments, however, indicate that δ should approach the same universal value $\delta_c \approx 0.2$ Å for both compounds as T_c goes to zero. The difference found in the δ_m values should again compensate for the quantum correction due to the nuclear dynamics.

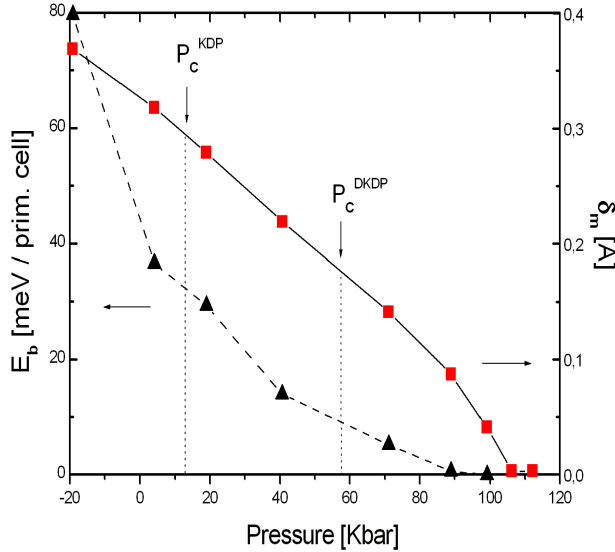


FIG. 9. Energy barrier E_b (triangles) and double-well minima separation δ_m (squares) as a function of pressure. Lines are guide to the eye only.

In fact, being lighter, protons will localize closer to the middle of the H-bond than deuteriums, leading in principle to such compensation. However, we will show below that this effect alone is not sufficient. The self-consistent geometrical effect discussed in the previous section, which was essential to explain the huge variation in the order parameter upon deuteration²⁹ is also crucial to explain the close similarity of δ_c for deuterated and protonated systems.

Neutron diffraction experiments indicate that, to have the same value of δ , different pressures have to be applied to KDP and DKDP.⁵² When converting pressures into global energy barriers using Fig. 9, the difference in energy barrier required to have the same value of δ turns out to be nearly independent of δ , assuming a value of ≈ 23 meV per unit cell (two formula units). This energy difference then seems to be a key quantity, which takes into account that the WF of the more-easily-tunneling protons in KDP will exhibit the same distance between peaks as the WF for deuterons in DKDP, only if the underlying double-well is significantly deeper, i.e. by 23

meV, and also the distance between minima δ_m is increased. The reason for this increased separation is in the very nature of the hydrogen bond: the more distant the O-atoms, the less covalent the bond, the larger δ_m , and the deeper the double-well. This is the essence of the geometrical effect, and 23 meV is the energy difference required to modify the O-O distance in such a way that the distance between peaks in the WF is the same for KDP and DKDP.

To show how the geometrical effect enters into play, we considered the feedback effective potential $V_{\text{eff}}(x)$ from Eq. 2. The probability distribution for the H(D) motion $|\Psi(x)|^2$, was obtained by solving the Schrödinger equation in the effective potential $V_{\text{eff}}(x)$. We chose the $N=7$ cluster, with the relation $\mu_D/\mu_H \approx 1.3$ for the effective masses in DKDP and KDP. The value of δ_m^0 was fixed to 0.24 Å. Within this model, we studied how the value of the energy barrier E_b^0 has to be modified (simulating the application of pressure), in order to keep the peak separation δ of the wave function $\Psi(x)$ constant upon deuteration. This study was carried out for different values of the non-linear parameter k in the model. Large values of k represent important feedback geometric effects.

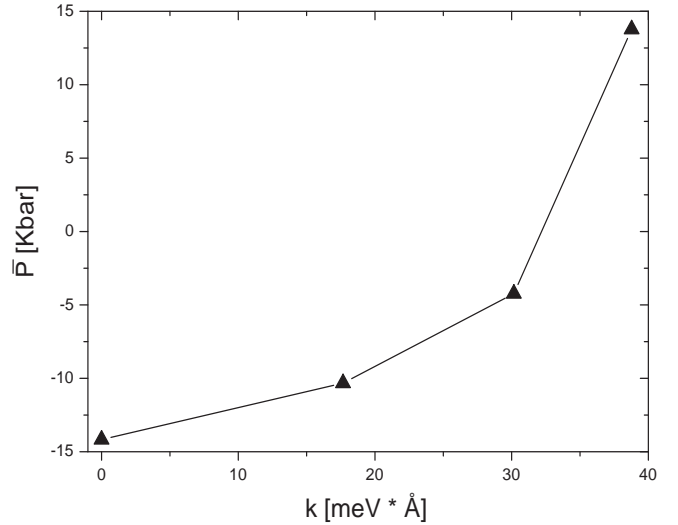


FIG. 10. Average pressure \bar{P} as a function of the coupling constant k from the non-linear model, as defined in text. Lines are guide to the eye only.

For each value of the non-linear parameter k , we searched for values of the barrier energies E_b^H and E_b^D for each isotope such that $\delta^{KDP} = \delta^{DKDP}$, with the additional constraint that the difference $E_b^H - E_b^D = 23$ meV remains constant. Using Fig. 9, we converted energy barriers into pressure, with the warning that these correspond to global energies, while E_b^0 represents cluster energy barriers. Since here we are interested in qualitative issues, the former is a reasonable approximation. Therefore, we calculate the average pressure $\bar{P} = \{P(E_b^H) + P(E_b^D)\} / 2$ for each value of k , which

serves to fix the absolute scale of pressures necessary to fulfill the above constraints. In Fig. 10 we plot \bar{P} as a function of k . For a value of $k = 0$ (no geometrical effect), in order to maintain δ constant upon deuteration, we have to apply a large negative pressure to the system, and hence expand it to have significantly higher energy barriers. Conversely, for larger pressures, as those experimentally measured, compensation can be achieved only by considering large values of k , thus leading to important structural non-linear effects. In summary, to explain pressure effects on KDP and DKDP,⁵² it is necessary to consider the non-linear relation between isotope substitution and geometric effect.

VII. DISCUSSION AND CONCLUSIONS

The nature of the instability that drives the FE transition and leads to the onset of the spontaneous polarization P_s has been extensively discussed in the past.^{10,57,45} Although the H(D) ordering in the basal plane is undoubtedly correlated with the transition, it was originally assumed that P_s , which is oriented along the c -axis, was due to the displacements of K^+ and P^- ions along this axis.¹⁰ However, the observed value of P_s can only be explained within this model if unrealistic, very large charges for the phosphorous ion are assumed.⁴⁵ Bystrov and Popova⁴⁵ proposed, alternatively, that the source of P_s could be the electron density shift in the P-O and P-O-H bonds in the polar direction, which occurs when the protons order perpendicularly. This assumption cannot be assessed through model calculations, for it is originated in the complex electronic interactions in the system.

By means of the present *ab initio* calculations we were able to overcome this limitation, and to show that the FE instability has its origin on an electronic charge reorganization within the internal P-O and P-O-H bonds of the phosphates, as the H-atoms order off-center in the H-bonds. As a matter of fact, the overall effect produced by the H-ordering is an *electronic charge flow* from the O2 side to the O1 side of the PO_4 tetrahedron, and a concomitant distortion of the former.²⁶ This is in agreement with the explanation given in Ref.⁴⁵, and also agrees with the results obtained by another recent first-principles calculation.²⁸

The microscopic origin of the global FE instability, i.e. the connection between H ordering and phosphate distortions, is also demonstrated in the strong correlation between the off-centering parameters δ for H and γ for K-P (see inset of Fig. 4). One of the observations here is that the overall potential for the H motion is not in fact separable, and one has to deal with the problem of the "chicken and the egg", what is really first?²² Nevertheless, using that γ is a measure of polarization, we showed that the source of the FE instability is in the H off-centering, and not vice versa.

There is a long controversy about the origin of the FE transition. Some experimental facts support the coupled proton-phonon model which displays essentially a displacive-like transition.⁵⁸ Other experiments, e.g. Raman studies⁵⁹, seem to indicate the importance of the order-disorder character of the transition originated in the H_2PO_4 unit dipoles. Electron-nuclear double-resonance (ENDOR) measurements⁶⁰ indicate that not only the H_2PO_4 group, but also the K atoms, are disordered over at least two configurations in the paraelectric phase. It is also shown by neutron scattering experiments that the P atom is distributed over at least two sites in DKDP.^{50,51} In spite of the still unresolved character of the transition, it is clear that local instabilities arising from the coupling of light and heavy ions are very important in this system, irrespective of the correlation length scale associated with the transition.

In fact, our calculations in the PE phase show that local proton distortions with the FE mode pattern need to be accompanied by heavy ion relaxations in the PO_4 -K group to produce significant instabilities, a fact which is in agreement with experiments. We have shown that the correlation length associated with the FE instability is much larger in KDP than in DKDP, suggesting that DKDP will behave more as an order-disorder ferroelectric than KDP.

The coherent interference of the proton in the two equivalent sites of the PE phase was observed recently by neutron Compton scattering experiments.¹⁴ Quantum coherence arises in our calculations for DKDP only when P and K ions are allowed to relax together with the deuterons. In KDP, the onset of tunneling and hence, coherence, would require relaxations of clusters comprising more than three KH_2PO_4 groups, which were not considered in the present work. The momentum distributions calculated in the PE phase are in qualitative agreement with the experiment.¹⁴ Quantum coherence would, thus, be produced by a dressed proton, i.e. strongly correlated with the heavier ions. In fact, in Ref.¹⁴, many-body effects due to the motion of the surrounding ions are not excluded, but it turns out that these are difficult to assess. We have also found good agreement with the experiment for the momentum distribution in the FE phase, which corresponds to a single, anharmonic well for each individual proton, in a host FE lattice. In this situation there is no coherence between the motions of the various protons.

The most striking feature, which is not yet satisfactorily understood, is undoubtedly the huge isotope effect in the critical temperature and the order parameter of the transition. The first explanation was that proposed by the tunneling model and later modifications,^{9,10} but soon after the vast set of experiments carried out by Nemes and co-workers,^{47,18,19,50,52} and the comprehensive structural compilation of Ichikawa *et al.*,¹⁶ the importance of the so-called geometrical effect as an alternative explanation became apparent. Other experiments^{59,15,14} and models^{11,23,13} favoured one or the other

vision, or even both, but an overall and consistent explanation of the phenomenon is still lacking. Still unanswered questions like: if tunneling occurs, what are the main units that tunnel?, what is the connection between tunneling and geometrical effects?, and what is the true microscopic origin of the latter?, are possibly some of the reasons why a full explanation of the isotope effect is not yet available. With the aid of the *ab initio* scheme, our efforts in this direction shed also light onto the underlying microscopic mechanism for the isotope effect.

Protons alone are not able to tunnel because the effective potentials in which they move display tiny double wells, and the particles are broadly delocalized around the center of the H-bonds. In this regard, we conclude that the simplified version of the tunneling model, i.e. that of a tunneling proton, or even a collective proton soft-mode alone, is not supported by our calculations. On the other hand, we observe "tunneling clusters", with an effective mass much larger than that of a single, or even several, protons (deuterons), due to the correlation with heavier ions. These clusters have different sizes, leading to different lengths and energy scales competing in the system in the PE phase. The smallest tunneling unit in DKDP is found to be the KD_2PO_4 group. This results agree with the idea developed by Blinc and Zeks of a tunneling model for the whole H_2PO_4 unit,⁶¹ which helped to describe the typical order-disorder phenomena observed in some experimental trends.⁵⁸ However, the explanation for the isotope effect arising in the present work is even more complex, and goes beyond the concept of "tunneling alone" as its main cause.

Although the PE phase of the system shows a complex scenario due to the appearance of different length scales, it is clear that larger clusters will prevail as the transition approaches. We have shown for both isotopes that tunnel splittings in these clusters at fixed potential are much smaller than the thermal energy at the critical temperature. Thus, at fixed potential, tunneling is not able to account for the large isotope effect in the system. However, as the dressed particle is delocalized by tunneling, the effective potential felt by the H(D)-atom changes upon isotopic substitution, due to significant modifications in the chemical properties of the O-H...O bond, which are reflected in a concomitant *lattice relaxation*.

With the aid of a simple model based in our *ab initio* results, we were able to show how this feedback effect strongly amplifies the geometrical modifications in the H(D)-bridge. Tunneling triggers a self-consistent mechanism, but in the end, the geometrical effect dominates the scenario and accounts for the huge isotope effect, in agreement with neutron scattering experiments.^{19,52} Therefore, these aspects, which were largely debated in the past, here appear as complementary and deeply connected to each other.^{11,57,29}

The feedback effect of the geometrical modifications on the proton distribution is also necessary to explain the results of experiments under pressure.⁵² There, it was observed that the critical pressures at which the transi-

tion temperature vanishes correspond to an isotope and material-independent value of the peak separation in the proton distribution. We have shown that this unique value for KDP and DKDP can be achieved only as a consequence of a compensation between quantum delocalization effects and geometrical modifications imposed by pressure.⁵³

The question of why T_c is so closely related to the distance between H peaks δ is still open. A possible explanation can rely on the fact that equal GS levels relative to the top of the barrier in a double well potential correspond to approximately equal δ , irrespective of the energy barrier height and mass of the tunneling particle. We have verified in test calculations that this holds as long as the GS energy is not very deep below the top of the energy barrier, which means not too low pressures, as discussed in Section VI. In addition, in our mean-field description of the scenario of the FE transition, T_c should be related to the energy difference between the GS level and the top of the barrier in the double well potential of a tunneling cluster (see Fig. 5). This could explain the close relation between T_c and δ observed in neutron diffraction experiments.⁵²

The nonlinear feedback between tunneling and structural modifications is a phenomenon of wider implications. Tunneling units are indeed observed in a large variety of molecular compounds and biomolecules. Both tunneling and structural changes are important for the reaction mechanisms of enzymes⁶² and other biological processes. Our results on KDP supports the already expressed need for revision of the general theories of host-and-tunneling systems.²²

In summary, we showed that proton ordering in KDP leads to an electronic charge redistribution and ionic displacements that originate the spontaneous polarization of the ferroelectric phase. The instability process is controlled by the hydrogen off-centering. The double-peaked proton distribution in the bridges, observed in the paraelectric phase, cannot be explained by a dynamics of protons alone. These must be correlated with displacements of the heavier ions within clusters. These tunneling clusters can explain the recent evidence of tunneling obtained from Compton scattering measurements. We also showed that the mere mass change upon deuteration does not explain the huge isotope effect observed. We find that structural changes arising from the modification of the covalency in the bridges produce a feedback effect on the tunneling that strongly enhances the phenomenon. The resulting influence of the geometric changes on the isotope effect is in agreement with experimental data from neutron scattering. Moreover, the behavior of the proton/deuteron distribution in the bridges under pressure can only be explained by invoking the mentioned feedback effect of geometry.

ACKNOWLEDGMENTS.

We thank E. Tosatti for helpful discussions. J. K. and G. C. thank C. Sánchez for valuable discussions. S. K. also acknowledges very useful discussions with N. Dalal and R. Blinc. R. M. and S. K. thank support from CONICET and ANPCyT (grant PICT99 03-07248), Argentina and from ICTP, Trieste, Italy. S. K. also thanks support from Fundación Antorchas, Argentina and the Florida State University (FSU), Tallahassee, USA. G. C. thanks the European Social Fund for funding. Part of the calculations have been done using the allocation of computer time of the UKCP consortium.

-
- ¹ R. Blinc and B. Zeks, in *Soft Modes in Ferroelectrics and Antiferroelectrics*, edited by E. P. Wohlfarth (North-Holland, Amsterdam, 1974).
 - ² M. E. Lines and A. M. Glass, *Principles and Applications of Ferroelectric and Related Materials* (Clarendon Press, Oxford, 1977).
 - ³ M. Benoit, D. Marx and M. Parrinello, *Nature* **392**, 258 (1998).
 - ⁴ S. T. Bramwell, *Nature* **397**, 212 (1999).
 - ⁵ D. J. Lockwood, N. Ohno, R. J. Nelmes and H. Arend, *J. Phys. C: Solid State Phys.* **18** L559 (1985).
 - ⁶ G. A. Samara and D. Semmingsen, *J. Chem. Phys.* **71** 1401 (1979).
 - ⁷ P. W. R. Bessonette and M. A. White, *J. Chem. Phys.* **110**, 3919 (1999).
 - ⁸ J. C. Slater, *J. Chem. Phys.* **9**, 16 (1941).
 - ⁹ R. Blinc, *J. Phys. Chem. Solids* **13**, 204 (1960).
 - ¹⁰ K. Kobayashi, *J. Phys. Soc. Jpn.* **24**, 497 (1968).
 - ¹¹ E. Matsushita and T. Matsubara, *Prog. Theor. Phys.* **67**, 1 (1982); T. Matsubara and E. Matsushita, *Prog. Theor. Phys.* **71**, 209 (1984).
 - ¹² M. Kojyo and Y. Onodera, *J. Phys. Soc. Jpn.* **57**, 4391 (1988).
 - ¹³ A. Bussmann-Holder and K. H. Michel, *Phys. Rev. Lett.* **80**, 2173 (1998); N. Dalal, A. Klymachyov and A. Bussmann-Holder, *ibid.* **81**, 5924 (1998).
 - ¹⁴ G.F. Reiter, J. Mayer and P. Platzman, *Phys. Rev. Lett.* **89**, 135505 (2002).
 - ¹⁵ S. Ikeda *et al.*, *J. Phys. Soc. Japan* **63**, 1001 (1994).
 - ¹⁶ M. Ichikawa, K. Motida and N. Yamada, *Phys. Rev. B* **36**, 874 (1987).
 - ¹⁷ Z. Tun *et al.*, *J. Phys. C: Solid State Phys.* **21**, 245 (1988).
 - ¹⁸ R.J. Nelmes, *J. Phys. C: Solid State Phys.* **21**, L881 (1988).
 - ¹⁹ M.I. McMahon *et al.*, *Nature (London)* **348**, 317 (1990).
 - ²⁰ J. Seliger and V. Žagar, *Phys. Rev. B* **59**, 13505 (1999).
 - ²¹ J.M. Robertson and A.R. Ubbelohde, *Proc. R. Soc. London A* **170**, 222 (1939).
 - ²² J.A. Krumhansl, *Nature (London)* **348**, 285 (1990).
 - ²³ H. Sugimoto and S. Ikeda, *Phys. Rev. Lett.* **67**, 1306 (1991).
 - ²⁴ H. Sugimoto and S. Ikeda, *J. Phys.: Condens. Matter.* **8**, 603 (1996).
 - ²⁵ D. Merunka and B. Rakvin, *Solid State Comm.* **129**, 375 (2004); *Phys. Rev. B* **66**, 174101 (2002).
 - ²⁶ S. Koval, J. Kohanoff, R. L. Migoni, and A. Bussmann-Holder, *Comput. Mater. Science* **22**, 87-93 (2001).
 - ²⁷ S. Koval, J. Kohanoff and R. L. Migoni, *Ferroelectrics* **268**, 239 (2002).
 - ²⁸ Q. Zhang, F. Chen, N. Kioussis, S. G. Demos and H. B. Radousky, *Phys. Rev. B* **65**, 024108 (2002).
 - ²⁹ S. Koval, J. Kohanoff, R. L. Migoni and E. Tossati, *Phys. Rev. Lett.* **89**, 187602 (2002).
 - ³⁰ C. S. Liu, N. Kioussis, S. G. Demos and H. B. Radousky, *Phys. Rev. Lett.* **91**, 015505 (2003).
 - ³¹ P. Hohenberg and W. Kohn, *Phys. Rev. A* **136**, 864 (1964).
 - ³² W. Kohn and L. J. Sham, *Phys. Rev. A* **140**, 1133 (1965).
 - ³³ P. Ordejón, E. Artacho and J.M. Soler, *Phys. Rev. B* **53**, R10441 (1996).
 - ³⁴ D. Sánchez-Portal, P. Ordejón, E. Artacho and J.M. Soler, *Int. J. Quantum Chem.* **65**, 453 (1997).
 - ³⁵ O.F. Sankey and D.J. Niklewsky, *Phys. Rev. B* **40**, 3979 (1989).
 - ³⁶ J.P. Perdew, K. Burke and M. Ernzerhof, *Phys. Rev. Lett.* **77**, 3865 (1996).
 - ³⁷ M. Tuckerman, D. Marx and M. Parrinello, *Nature* **417**, 925 (2002).
 - ³⁸ A. D. Becke, *Phys. Rev. A*, **38**, 3098 (1988); C. Lee, W. Yang, and R. Parr, *Phys. Rev. B* **37**, 785 (1988).
 - ³⁹ N. Troullier and J.L. Martins, *Phys. Rev. B* **43**, 1993 (1991).
 - ⁴⁰ Baroni S., de Gironcoli S., dal Corso A. and Gianozzi P. *Rev. Mod. Phys.* **73**, 515 (2001).
 - ⁴¹ R.J. Nelmes, Z. Tun and W.F. Kuhs, *Ferroelectrics* **71**, 125 (1987).
 - ⁴² S. Scheiner, in *Proton transfer in hydrogen-bonded systems*, ed. T. Bountis, NATO ASI series B, v. **291** (Plenum, New York, 1992).
 - ⁴³ A. R. Grimm, G. B. Bacskey and A. D. J. Haymet, *Mol. Phys.* **86**, 369 (1995).
 - ⁴⁴ T. R. Dyke, K. R. Mack and J. S. Muentner, *J. Chem. Phys.* **66**, 498 (1977).
 - ⁴⁵ D. S. Bystrov and E. A. Popova, *Ferroelectrics* **72**, 147 (1987).
 - ⁴⁶ G. Colizzi, PhD Thesis (unpublished).
 - ⁴⁷ R. J. Nelmes, *Ferroelectrics* **71**, 87 (1987).
 - ⁴⁸ R. J. Nelmes *et al.*, *J. Phys. C: Solid State Phys.* **18**, L711 (1985).
 - ⁴⁹ The minimum size leading to a tunneling state below the central barrier is a measure of the crossover length to a quantum dominated FE transition.
 - ⁵⁰ M.I. McMahon *et al.*, *Europhys. Lett.* **13**, 143 (1990).
 - ⁵¹ M.I. McMahon *et al.*, *Ferroelectrics* **124**, 351 (1991).
 - ⁵² R. J. Nelmes *et al.*, *Ferroelectrics* **124**, 355 (1991).
 - ⁵³ G. Colizzi, J. Kohanoff, J. Lasave, S. Koval and R.L. Migoni, *Ferroelectrics* (in press).
 - ⁵⁴ D. Vanderbilt, *Phys. Rev. B* **41**, 7892 (1990).
 - ⁵⁵ Endo S. *et al.*, *Solid State Commun.* **112**, 655 (1999).
 - ⁵⁶ G. A. Samara, *Ferroelectrics* **5**, 25 (1973).
 - ⁵⁷ R. Blinc and B. Zeks, *Ferroelectrics* **72**, 193 (1987).
 - ⁵⁸ See for instance, M. Tokunaga and T. Matsubara, *Ferro-*

electrics **72**, 175 (1987); and references therein.

⁵⁹ Y. Tominaga *et al.*, Solid State Commun. **47**, 835 (1983);

Y. Tominaga *et al.*, Solid State Commun. **48**, 265 (1983)

⁶⁰ B. Ravkin and N. S. Dalal, Phys. Rev. B **44**, R892 (1991).

⁶¹ R. Blinc and B. Zeks, J. Phys. **C15**, 4661 (1982).

⁶² A. Kohen, R. Cannio, S. Bartolucci and J. P. Klinman, Nature **399**, 496 (1999).